Synthesis, preparation, and conformation of stimulus-responsive end-grafted poly(methacrylic acid-*g*-ethylene glycol) layers

Miao Ye, Dong Zhang, Lin Han, Jonathon Tejada and Christine Ortiz*

Received 1st August 2005, Accepted 4th January 2006
First published as an Advance Article on the web 3rd February 2006
DOI: 10.1039/b510894b

Here we report the formation of stimulus-responsive chemically end-grafted ''brush-brushes'' by synthesizing, mono thiol(end)-functionalized poly(methacrylic acid-*g*-ethylene glycol) or poly(MAA-*g*-EG) comb-type graft copolymers *via* a combination of protecting group chemistry and atom transfer radical polymerization using the initiator 2-(2,4-dinitrophenylthio)ethyl 2-bromo-2-methyl propionate. The polymers were synthesized with three different molecular weights (15 k, 17 k and 27 k), PEG side chain graft densities (EG/MAA mole ratio = 2.2, 0.4 and 1.9, respectively), and a PEG molecular weight = 1100 and then chemically end-grafted to gold substrates *via* chemisorption, resulting in molecular separation distances of ~3–4 nm. pH-Dependent swelling was confirmed to take place gradually above pH 4–5 and quantified by heights measured by contact mode AFM imaging of microcontact printed (μCP) samples. Swelling factors (maximum height/minimum height) were fairly large (3.6–7.3) and a decrease in molecular weight by ~2× and side chain graft density by ~4× resulted in a decrease in swelling factor by ~2×. Layer height *versus* normal force for all three polymers measured by contact mode atomic force microscope imaging on μCP samples at pH 9 showed a nonlinearly decreasing relationship and complete compression ~<2 nm for forces >10 nN. At pH 4, all polymer layers were largely collapsed (heights ~<4 nm) and incompressible (*i.e.*, heights were independent of normal force).

Introduction

Surfaces with reversible stimulus-responsive interfacial properties have great promise in a variety of applications including, for example: drug delivery, transport, separation, and detection of biomolecules, directed cellular function, controlled adhesion, friction, and lubrication in microfluidics, and force generation in micro- and nanoscale devices. Surface bound stimulus responsive polymers (sometimes called environmentally responsive or ''smart'' polymers) are ideal candidates for many of these applications given that they may be conformationally sensitive to a wide variety of parameters (*e.g.*, solvent quality, pH, ionic strength, type of salt, light, temperature, and electrical potentials) and the fact that this sensitivity can be tailored by chemical structure, molecular weight, composition, and architecture.[1–5] In order to employ such systems for the above mentioned applications, control of the magnitude of the stimulus response, the range over which it takes place, the response time, the reversibility, and hysteresis will be critical.

In this paper, we have synthesized comb-type graft copolymers of poly(methacrylic acid-*g*-ethylene glycol) or poly(MAA-*g*-EG) in mono (thiol)end-functionalized form and then chemically end-grafted them to planar substrates to prepare surface-bound stimulus responsive ''brush–brushes'' (Fig. 1). Comblike side-chain graft copolymers, also called molecular bottle brushes, cylindrical brushes, or polymacromonomers, are branched macromolecules composed of an array of side chains attached to a main chain backbone. Many types have been synthesized (see, for example, refs 6–9) and also exist in biology; *e.g.* cartilage aggrecan[10] and epithelial mucins.[11] The synthesis and stimulus responsive nature of poly(MAA-*g*-EG) without end-functionalization has been reported previously by free radical polymerization[12–14] and by atom transfer radical polymerization (ATRP).[15] High molecular weight systems (~700–800 K) free in solution show a dramatic conformational transition in aqueous solution from a collapsed hydrophobic intrapolymer complex at low pH to an expanded hydrophilic coil at high pH that is essentially completed for pH > 6.0 and is amplified compared to the poly(methacrylic acid) or PMAA homopolymer.[14] Since many of the potential applications described previously necessitate polymers bound to surfaces in a well defined manner, the methodology presented here for end-functionalization and chemical end-grafting of poly(MAA-*g*-EG) provides a technologically important model system that then can be used for studies of macromolecular surface properties, such as nanoscale conformation and wettability. We are particularly interested in employing these end-grafted poly(MAA-*g*-EG) layers for precise control of normal and lateral nanomechanical surface properties (*i.e.*, the form of the attractive or repulsive intersurface potential, the lateral proportionality coefficient between normal and shear forces) both of which will be reported in a separate publication.[16] In addition, end-grafted systems with unique macromolecular architectures, such as combs, are expected to undergo interesting new stimulus responsive and nanomechanical behavior at high

Department of Materials Science and Engineering, Massachusetts Institute of Technology, 77 Massachusetts Avenue, Cambridge, Massachusetts, 02139, USA. E-mail: cortiz@mit.edu

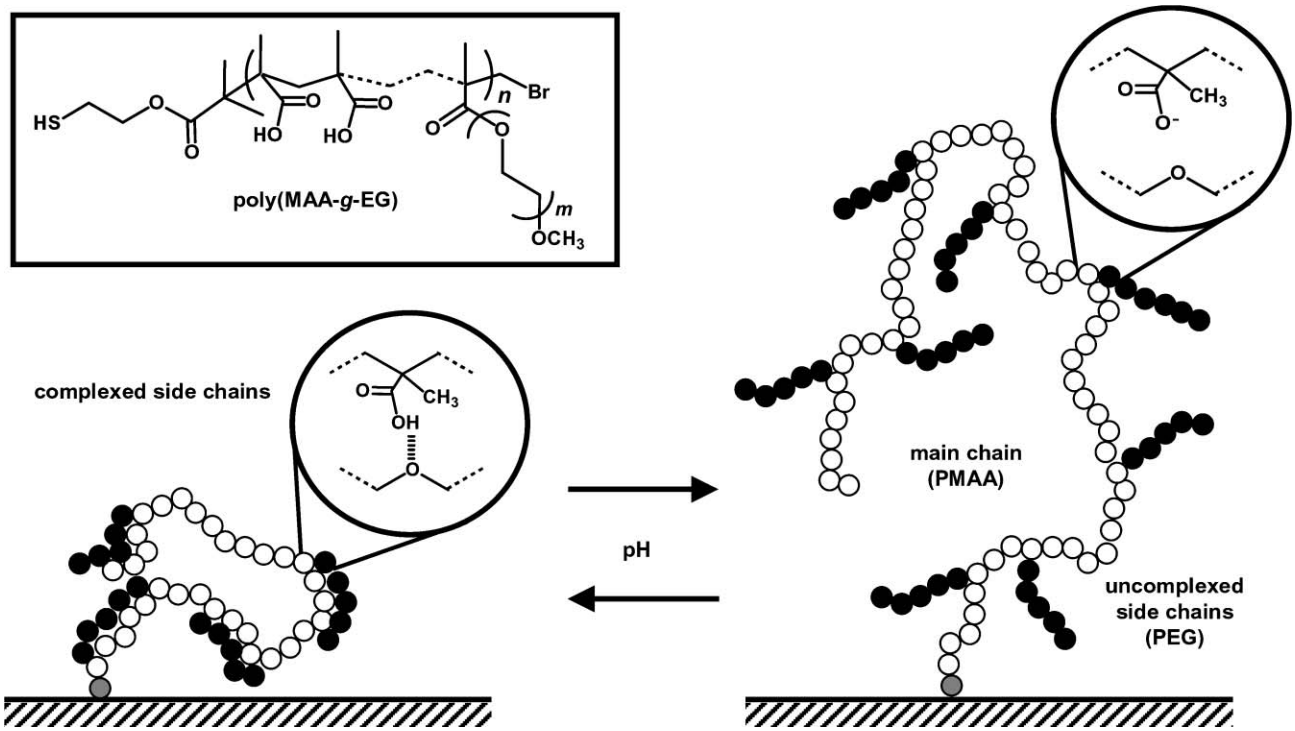

Fig. 1 Schematic of a conformational transition of a chemically end-grafted stimulus-responsive side-chain graft copolymer (insets show molecular interactions for poly(MAA-*g*-EG)).[12–14]

enough surface grafting densities due to lateral intermolecular interactions and confinement (for example, between PEG side chains of the poly(MAA-*g*-EG)), which are expected to stiffen the layer. This concept is employed in cartilage aggrecan *via* glycosaminoglycan side chain interactions and has important physiological consequences.[17,18] Experiments which probe the nanoscale stimulus responsiveness of end-grafted poly(MAA-*g*-EG) also have the potential to provide important fundamental scientific information on the molecular origins of the unique macroscopic equilibrium swelling behavior of cross-linked hydrogels based on this graft copolymer.[19]

Three mono(thiol)end-functionalized forms of poly(MAA-*g*-EG) with varying macromolecular architecture were synthesized by combining protecting group chemistry[20] with ATRP, using an alternate initiator[21–23] than that reported previously.[15] The number average molecular weights of these polymers were 15 k, 27 k, and 17 k with side chain graft densities ~8–9% of the total main chain backbone monomers (EG/MAA molar ratio ~ 2) for the 15 k and 27 k and a side chain graft density of ~1.9% (EG/MAA molar ratio ~ 0.4) for the 17 k. Characterization was achieved by gel permeation chromatography (GPC), ^{1}H nuclear magnetic resonance (NMR), and Fourier transform infrared spectroscopy (FTIR). The polymers were chemically end-grafted to planar Au-coated substrates using a "grafting to" chemisorption technique (which yielded molecular surface separation distances of ~3–4 nm) and then characterized by contact angle measurements to monitor the kinetics of chemisorption and assess wettability. Samples were prepared *via* the technique of micro-contact printing (μCP)[24] where patterned surfaces with micrometre-sized areas of the end-grafted polymers were surrounded by areas of a neutral hydroxyl-terminated self-assembled monolayer (OH-SAM). The relative graft copolymer layer height was measured as a function of pH in aqueous solution using these patterned samples by contact mode atomic force microscopy (AFM) imaging,[17] thus providing direct information on the nature of the pH-dependent conformational transition.

Experimental

Materials

2,4-Dinitrofluorobenzene (99%), 2-mercaptoethanol (98%), 2-bromoisobutyryl bromide (98%), *tert*-butyl methacrylate (BMA) (98%), poly(ethylene glycol) methyl ether methacrylate (MW ~ 1100 g mol^{-1}, 23 EG monomers long), triethylamine (99.5%), chloroform (99.8% A.C.S. Reagent), toluene (99.8%, HPLC grade), 2,2′-dipyridyl (99%), copper(I) bromide (99.999%), chloroform-*d* (100.0%), methanol-d_4 (99.8%), tris-(hydroxymethyl) aminomethane (Tris), 4-morpholineethanesulfonic acid monohydrate (MES), acetic and formic acid were all purchased from Sigma-Aldrich. All water used for solutions, rinsing, and storage was deionized (DI, pH 5.6, 18 MΩ cm resistance). (100) N-Type Silicon wafers were purchased from Crystaltek. Chromium was purchased from R.D. Mathis (Long Beach, CA USA) and gold (99%) was purchased from J & J Materials (Neptune City, NJ USA). All the other chemicals were used as received from commercial suppliers.

Synthesis of HS-poly(*tert*-BMA-*g*-EG)

The synthesis of the thiol-protected initiator: 2-(2,4-dinitrophenylthio)ethyl 2-bromo-2-methyl propionate (DEBPM) was

performed as described previously.[20] In a typical polymerization (Fig. 2), a 250 ml three-neck round bottom flask was equipped with a condenser, argon inlet and paddle stirrer. 0.078 g (0.0005 mol) of 2,2′-dipyridyl and 0.029 g (0.0002 mol) of CuBr were added to the mixture of 14.2 g (0.1 mol) of *tert*-butyl methacrylate, 1.1 g (0.001 mol) of poly(ethylene glycol) methyl ether methacrylate (MW ~ 1100) and 12.0 g of methanol. Then, 0.078 g (0.0002 mol) of 2-(2,4-dinitophenylthio) ethyl 2-bromo-2-methylpropionate was added into the solution. The solution was purged with Argon to remove oxygen. The ratio of catalyst–initiator–ligand was 1 : 1 : 2.5. The molar ratio of *tert*-butyl methacrylate and poly(ethylene

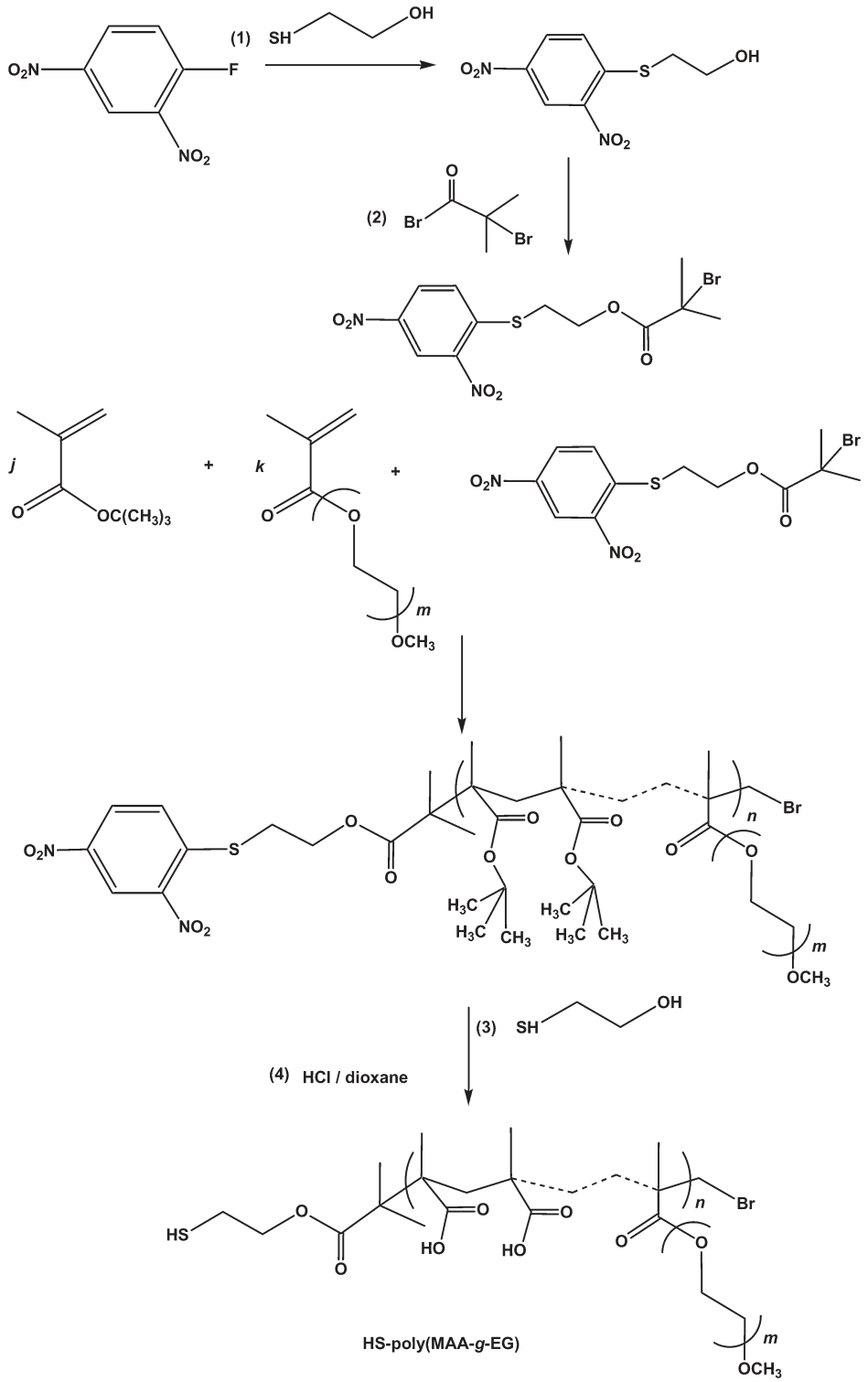

Fig. 2 Atom transfer radical polymerization chemical reaction scheme for synthesis of mono thiol(end)-functionalized poly(methacrylic acid-*g*-ethylene glycol) or HS-poly(MAA-*g*-EG).

glycol) methyl ether methacrylate was 100 : 1. The solution was heated to 40 °C and maintained at this temperature with stirring under argon for 17 h in the synthesis of the 15 k polymer. The amount of the initiator, ligand, and catalyst were doubled in the synthesis of the 17 k polymer while the molar ratio of *tert*-butyl methacrylate and poly(ethylene glycol) methyl ether methacrylate was 50 : 1 and the reaction temperature was 60 °C in the synthesis of the 27 k polymer. The crude thiol-protected polymer was obtained in solid form and purified by dissolving in hot methanol, cooling, and precipitating in DI water. The polymer was then filtered and dried in a vacuum oven at 50 °C overnight. Then, the thiol-protected polymer was rinsed again with DI water, petroleum ether, cyclohexane, and filtered and dried in a vacuum oven at 50 °C overnight. In a 20 mL borosilicate glass scintillation vial, 1.00 g of thiol-protected polymer, 5.2 g of mercaptoethanol, 0.1 g of triethylamine and 0.8 g of DI water were added and stirred by a magnetic stirrer at room temperature for 17 h. The polymer was then precipitated by adding DI water, filtered, and dried in a vacuum oven at 50 °C overnight. For further purification, the HS-poly(*tert*-BMA-*g*-EG) was dissolved in methanol and fractioned by adding water or petroleum ether. The polymer was filtered and dried at 50 °C in a vacuum oven overnight to yield purified HS-poly(*tert*-BMA-*g*-EG).

Conversion of HS-poly(*tert*-BMA-*g*-EG) to HS-poly(MAA-*g*-EG)

The cleavage of the *tert*-BMA groups of the HS-poly(*tert*-BMA-*g*-EG) was achieved by treatment with an HCl solution in dioxane. In a 50 mL single-neck round bottom flask 0.6 g of HS-poly(*tert*-BMA-*g*-EG) were suspended in 20 mL dioxane. 3 mL of a concentrated HCl solution (37%) were added and the mixture was magnetically stirred at 80 °C for 5 h. Then, most of the solvent was evaporated, the polymer was precipitated and rinsed with cyclohexane, and then dried at 50 °C in a vacuum oven overnight to yield HS-poly(MAA-*g*-EG).

Polymer characterization

GPC was taken using DAWN from Wyatt Technology (Santa Barbara, CA USA), a Waters (Milford, MA USA) 510 HPLC pump and Waters 410 Differential Refractometer to measure the weight average molecular weight, M_w, and the molecular weight distribution. The calibration curves for polystyrene and poly(methyl methacrylate) were determined in tetrahydrofuran (THF). The polymers were prepared in a 5 mg mL^{-1} solution of THF. ^1H NMR spectra were obtained on Varian Unity-300 and Varian Mercury-300 (Palo Alto, CA USA) in chloroform-*d* or methanol-d_4. The chemical shifts (δ) of hydrogen atoms of chloroform-*d* or methanol-d_4 were used for reference. From the integrated peak areas corresponding to protons of the protecting end-group and the characteristic chemical groups of the poly(ethlyene glycol) or PEG and PMAA, the number average molecular weight, M_n, and grafting density of the copolymer were calculated, as described previously.[20,25] FTIR spectra were obtained on Nicolet (now Thermo Electron Corporation, Waltham, MA USA) Magna 860 Fourier Transform Infrared Spectrometer in air. The polymers were mixed with KBr and compressed into pellets. Both the copolymer and KBr were dried in vacuum oven at 50 °C overnight to remove moisture before running FTIR. Qualitative (visual) solubility assessment was performed after mixing 0.005 g of the polymers with ~10 ml of buffer solutions (pH4 formate, pH5 acetate, pH6 MES and pH 7.1–9 Tris and stirring for ~1 h.

End-grafting of HS-poly(MAA-*g*-EG) to planar surfaces

Gold-coated silicon substrates were prepared as previously described[26] and cleaned using a piranha solution (98% H_2SO_4–30% H_2O_2, volume ratio 3 : 1) for 10 min followed by copious rinsing with water, acetone, and methanol. Any terminal disulfide bonds formed by the –SH end groups of HS-poly(MAA-*g*-EG) were reduced to a thiol group by diluting polymer to 200 μg mL^{-1} of methanol solution in 0.1 mM dithiothreitol (DTT, Sigma Aldrich) and incubating under continuous stirring for 1 h. After removal of the excess reactants using centrifugal filters (Centricon, Millipore, Billerica MA USA, 3000 MW cutoff), the Au substrates were immersed in 0.4 mg mL^{-1} of the polymer solution in methanol for times ranging between 3 and 72 h. The end-grafted poly(MAA-*g*-EG) surfaces were rinsed with acetone, methanol, and water thoroughly before experimentation.

Characterization of end-grafted poly(MAA-*g*-EG)

Advancing contact angles for the end-grafted poly(MAA-*g*-EG) layers were measured using droplets of ~0.5 ml DI H_2O and a VCA2000 Video Contact Angle system (AST Products, Inc., Billerica, Massachusetts, USA). The contact angle reported is the average of measurements on three different sample locations.

The polymer layer heights (and hence, macromolecular conformation) were measured in aqueous buffer solutions using μCP samples[24] in conjunction with contact mode AFM imaging.[17] The advantages and disadvantages of this technique have been discussed previously.[17] The patterned samples were prepared with micrometre-sized areas of the end-grafted poly(MAA-*g*-EG) surrounded by areas of a neutral hydroxyl-terminated self-assembled monolayer (OH-SAM) as shown in Fig. 3. A polydimethylsiloxane stamp with parallel lines 1.5 μm in width was compressed onto piranha-cleaned Au substrates using 1 mM ethanol solution of 11-mercaptoundecanol, $HS(CH_2)_{11}OH$ (Sigma-Aldrich), to fill the areas outside of the lines. Then the patterned substrate was immersed into a DTT-treated poly(MAA-*g*-EG) solution of 0.4 mg mL^{-1} for 72 h to allow the polymer to chemisorb to the inner areas of the lines. The samples were rinsed thoroughly with methanol, ethanol, and DI water prior to experimentation. Height maps were taken as a function of pH using these samples by contact mode atomic force microscopy (AFM) imaging in 0.005 M ionic strength (IS) buffered aqueous solution as a function of pH. The pH 4, pH 5 and pH 6 buffer solutions were formate, acetate, and MES, respectively, while pH 7.1, pH 8 and pH 9 were Tris. All buffer solutions used sodium chloride to adjust the ionic strength to 0.005 M. A Multimode Nanoscope III AFM (*Veeco*, Santa Barbara, CA USA) was used at the lowest normal imaging force possible ~200 pN (scan size = 10 μm, scan rate = 1 Hz, 256 datapoints per line

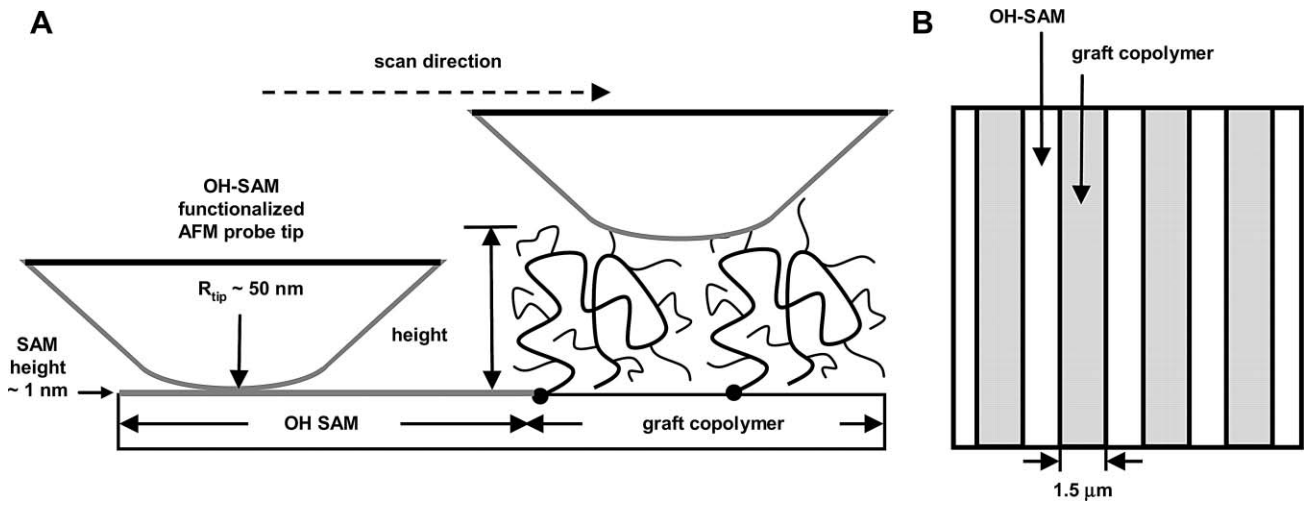

Fig. 3 (a) Side view schematic of height measurement using atomic force microscope contact mode imaging on micro contact printed surface of graft copolymer and hydroxyl-terminated self-assembled monolayer (OH-SAM) where R_{tip} is the probe tip end radius, and (b) schematic of top view of microcontact printed surface (adapted from ref. 17).

scan, and scan angle = 0°) with an OH-SAM functionalized cantilever probe tip prepared in the same manner as for the planar substrates (*Veeco*, end radius ~50 nm, nominal cantilever spring constant, $k \sim 0.06$ N m^{-1}). The AFM images were flattened and the polymer heights reported are the relative height between the OH-SAM surface areas outside the patterned lines (which have a height of ~1.4 nm in air[27]) and the polymer-functionalized surface areas within the patterned lines. The heights are the average of eight scan lines per image.

The micro-contact printed samples were gently dried in a stream of nitrogen and imaged using contact mode AFM and an OH-SAM functionalized cantilever probe tip in ambient conditions to measure the relative height in air using similar procedures as described above for the wet heights.

The polymer layer thickness in air was also measured on M-2000D Spectroscopic Ellipsometer (J. A. Woollam Co., Inc., Lincoln, NE USA). The change in polarization state of light reflected from the surface of the sample was measured *via* the ellipsometric values Ψ and Δ *versus* wavelength (200–1000 nm) at a fixed angle of incidence (70°) between the incoming beam and the sample surface normal. The polymer layer thickness was obtained by fitting the ellipsometry data with a Lorentz oscillator model over the wave length of 400–800 nm. The polymer layer surface was modeled as two layers: gold and the polymer. The thickness was fitted as the value with a mean squared error (MSE) less than five and was the average of the measurements at three different sample locations.

The surface grafting density, Γ (chains nm^{-2}), was calculated from the dry polymer layer height data as follows:

$$\Gamma\left(\frac{\text{chains}}{\text{nm}^2}\right) = \frac{\text{dry height(nm)}\rho\left(\frac{\text{g}}{\text{nm}^3}\right)6.023\times10^{23}\text{mol}^{-1}}{M_n\left(\frac{\text{g}}{\text{mol}}\right)}$$

In the dry state, the density of the polymer layer, ρ, was assumed to be the same as its bulk density. The densities of PMAA and PEG are known to be 1.0153 g cm^{-3} and 1.1135 g cm^{-3}, respectively.[28] The density of the copolymer was assumed to be an additive function of the densities of two compositional homopolymers on a weight basis (~1.07 g cm^{-3}).

Results and discussion

(A) Synthesis: Initiator and polymer characterization

The synthesis of poly(MAA-*g*-EG) without end-functionalization has been reported previously by free radical polymerication[12–14] and by ATRP.[15] To our knowledge the synthesis of thiol(end)-functionalized poly(MAA-*g*-EG) has never been reported before. It is known that controlled polymerization of methacrylic acid *via* ATRP is difficult because the acid monomers can poison the catalysts by coordinating to the transition metal and nitrogen-containing ligands can be protonated interfering with the metal complexation ability.[29] Alternatively PMAA can be obtained by polymerization of protected polymers such as *tert*-butyl methacrylate (*t*BMA). Reported ATRP formulation for polymerization of *t*BMA includes methyl 2-bromopropionate (initiator) and Cu(I)Br/*N*,*N*,*N*′,*N*″,*N*″-pentamethyldiethylenetriamine (PMDETA) or 2,2′-bipyridine (bpy) (catalyst) in bulk, methanol or methanol–water mixture;[30] *p*-toluenesulfonyl chloride (*p*-TsCl) (initiator) and Cu(I)Cl/*N*,*N*,*N*′,*N*″,*N*″-hexamethyltriethylenetetramine (HMTETA) (catalyst) in 50 vol.% anisole[31] or methyl ethyl ketone (MEK).[32] ATRP formulation for polymerization of poly(ethylene glycol) methyl ether methacrylate (PEGMEM) can be Cu(I)Cl/bpy or pyridyl methanimine-based ligands with various initiators in water;[33,34] a water soluble bromo-capped oligo(ethylene glycol) based alkyl initiator, Cu(I)Br with bpy, PMDETA, or HMTETA in water;[35] 1,2-dihydroxy-propane-3-oxy-(2-bromo-2-methylpropionyl) (initiator) and Cu(I)Br/*N*-(*n*-alkyl)-2-pyridylmethanimine in water;[36] ethyl 2-bromoisobutyrate (EtBriBu) or *p*-TsCl (initiator) and Cu(I)Br/4,4′-di(5-nonyl)-2,2′-bipyridyne (dNbpy) (catalyst) in toluene or THF.[37] Block copolymers of poly(ethylene glycol)-*b*-poly(*t*BMA) were also reported to be synthesized *via* ATRP

using PEG macroinitiator and Cu(I)Br/PMDETA in bulk[38] or THF.[15,39] Block copolymers of poly(ethylene glycol) with *n*-butyl methacrylate were prepared using PEG macroinitiator and Cu(I)Br/HMTETA in bulk;[40] poly(methyl methacrylate-co-poly(ethylene glycol) monomethacrylate) was synthesized using TsCl and CuBr/dNbpy in cyclohexanol or diphenyl ether.[41]

As a multicomponent system, initiator, catalyst including ligands, solvent and temperature of an ATRP reaction must all be taken into consideration. Based on the thiol protective group chemistry utilized[22] and our previous work on the ATRP synthesis of thiol end-functionalized poly(2-hydroxyethyl methacylate-*g*-ethylene glycol),[20] we chose the current ATRP formulation and obtained the thiol functionalized comb-type polymer.

^{1}H NMR, GPC, and solubility. The structure of the initiator, 2-(2,4-dinitrophenylthio)ethyl 2-bromo-2-methyl propionate, was verified by ^{1}H NMR (chloroform-*d*, δ): 9.11–9.10 (d, 1H), 8.48–8.44 (dd, 1H), 7.84–7.81 (d, 1H), 4.50–4.45 (t, 2H), 3.43–3.38 (t, 2H), and 1.96 (s, 6H) (*spectrum not shown*). Fig. 4a shows the ^{1}H NMR spectrum of the protected thiol-functionalized poly(*tert*-BMA-*g*-EG) in methanol-d_4. The three peaks at δ 9.08, 8.54 and 8.03 were attributed to the

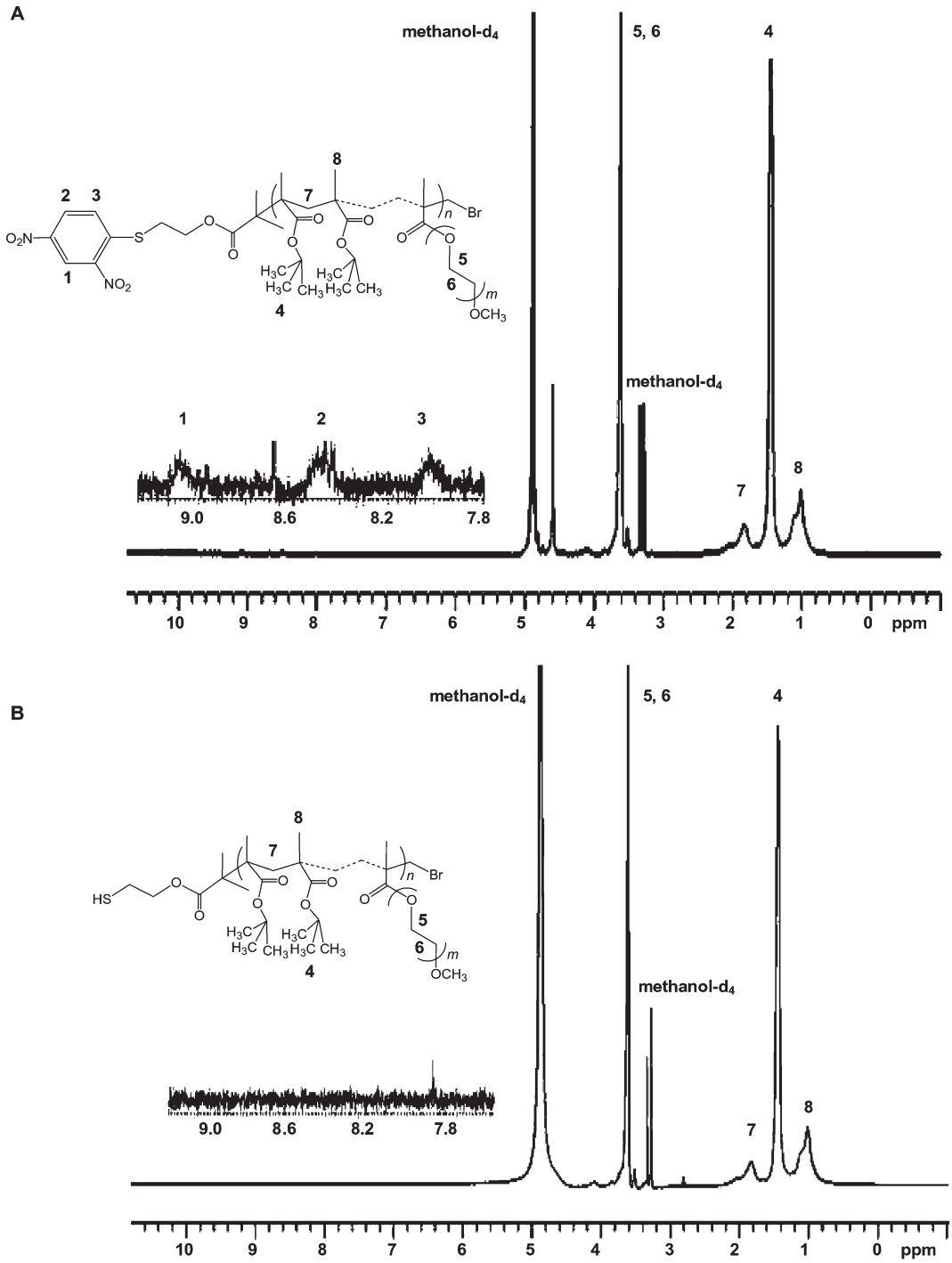

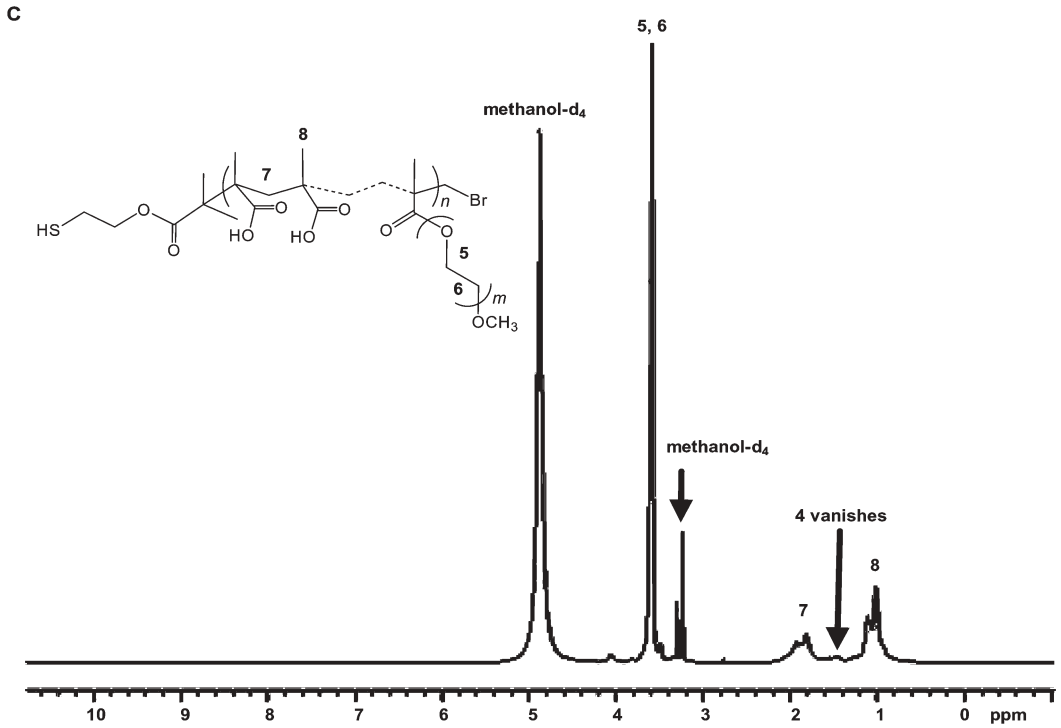

Fig. 4 ^{1}H Nuclear magnetic resonance (NMR) spectra in methanol-d_4 of (a) protected mono thiol(end)-functionalized poly(*tert*-butyl methacrylate-*g*-ethylene glycol) or poly(*tert*-BMA-*g*-EG)$_{20k}$, (b) mono thiol(end)-functionalized HS-poly(*tert*-BMA-*g*-EG)$_{20k}$, and (c) mono thiol(end)-functionalized poly(methacrylic acid-*g*-ethylene glycol) or HS-poly(MAA-*g*-EG)$_{15k}$. The numerical subscript in the abbreviated polymer name labels refer to the number average molecular weight, M_n, of the graft copolymer in g mol^{-1} (as measured by ^{1}H NMR) and "k" is an abbreviation for 1000. The peak numbers labeled in each NMR spectrum correspond to the protons labeled in the chemical structure insets at the top of each NMR spectrum.

Table 1 Parameters describing the macromolecular architecture of the thiol-protected poly(*tert*-butyl methacrylate-*g*-ethylene glycol) or poly(*tert*-BMA-*g*-EG) graft copolymers as determined by ^{1}H nuclear magnetic resonance (NMR) in methanol-d_4 and gel permeation chromatography (GPC) in tetrahydrofuran (THF). The numerical subscript in the abbreviated polymer name labels refer to the number-average molecular weight, M_n, of the graft copolymer in g/mol and "k" is an abbreviation for 1000, M_w is the weight average molecular weight measured by GPC, MW_{PEG} is the known molecular weight of each PEG chain, the PEG graft density (%) is defined as N_{PEG} divided by the total number of backbone monomers, N_{PEG} is the average number of PEG chains per poly(*tert*-BMA) or PMAA chain, DP_n is the number-average degree of polymerization, EG/*tert*-BMA (mole ratio) is calculated as the DP_n(EG)/DP_n(*tert*-BMA) = DP_n(EG)/DP_n(MAA), and $L_{contour}$ is the average contour length calculated from the known molecular weights assuming *ttt* conformations for the poly(methacrylic acid) or PMAA and *ttg* conformations for the PEG. The M_n of corresponding thiol-terminated poly(methacrylic acid-*g*-ethylene glycol) or HS-poly(MAA-*g*-EG) copolymers were calculated after removal of the *tert*-butyl groups and replacement with H atoms

	Thiol-protected poly(*tert*-BMA-*g*-EG)$_{20k}$	Thiol-protected poly(*tert*-BMA-*g*-EG)$_{35k}$	Thiol-protected poly(*tert*-BMA-*g*-EG)$_{25k}$
^{1}H NMR (methanol-d_4)			
M_n	19 900	35 200	25 300
EG/*tert*-BMA (mole ratio)	2.2	1.9	0.4
PEG graft density (%)	8.8	7.7	1.9
M_n (tBMA)	11 400	21 300	22 000
DP_n (*tert*BMA)	80	150	155
M_n (EG)	8500	13 800	3300
DP_n (EG)	176	286	67
MW_{PEG} (each side chain)	~1100	~1100	~1100
N_{PEG}	7.8	12.6	3.0
$L_{contour}$, main chain/nm	22.1	41.1	39.8
$L_{contour}$, side chain/nm	6.7	6.7	6.7
M_n after hydrolysis (calculated)	15 400 (HS-poly(MAA-*g*-EG)$_{15k}$)	26 800 (HS-poly(MAA-*g*-EG)$_{27k}$)	16 600 (HS-poly(MAA-*g*-EG)$_{17k}$)
GPC (THF)			
M_w	12 700	16 800	13 200
M_w/M_n	1.189	1.178	1.262
Solubility (aqueous solution)	Complete dissolution: pH 6–9 Swell: pH 4–5	Complete dissolution: pH 6–9 Swell: pH 4–5	Complete dissolution: pH6–9 Partial dissolution: pH 5 Swell: pH 4
Packing density, Γ (molecular separation distance)	0.071 chains nm^{-2} (~3.8 nm)	0.053 chains nm^{-2} (~4.3 nm)	0.109 chains nm^{-2} (~3.1 nm)
Contact angle (DI water, pH5.6) Instantaneous advancing	47 ± 2.6°	32 ± 0.6°	44 ± 2.4°
Instantaneous receding	11 ± 0.6°	0°	5 ± 0.5°

protons at positions 1, 2 and 3 from the 2,4-dinitrophenyl protecting group as shown in the chemical structure inset of Fig. 4a. The integrated areas of the peaks corresponding to positions 1, 2, and 3 were found to be approximately equivalent. The peaks at δ 4.87 and 3.31 correspond to methanol-d_4. The peak at δ 3.61 was attributed to the protons at positions 5 and 6 from the PEG graft side chains. The peak at δ 1.44 was attributed to the protons at position 4 from the methyl groups of *tert*-butyl methacrylate segments,[32] and the peaks at δ 1.9 and 1.0 were attributed to the protons from the methyl and methylene groups on the backbone. The peak at δ 4.7 may come from the protons on the C=C bonds of some residual monomers which still remained after purification. Table 1 shows the results of calculations to determine the macromolecular architectural parameters from the NMR data (performed as described previously[20,25]) compared with GPC data. The molecular weights were found to be 20 K, 25 K, and 35 K with PEG graft densities of 8.8, 1.7, and 1.9%, respectively corresponding to EG/*tert*-BMA mole ratios of 2.2, 1.9, and 0.4. The estimated average contour lengths of the main chain backbone (calculated from the molecular weights) for the three polymers were $\sim$22 nm (20 K), 41 nm (35 K), and 40 nm (25 K) (assuming *ttt* backbone conformations) and for the PEG side chains $\sim$7 nm (assuming *ttg* backbone conformations, which is known to exist in aqueous solution[42]).

After removal of the 2-(2,4-dinitrophenyl) protecting group, the characteristic end group peaks at positions 1, 2 and 3 vanished as shown in Fig. 4b, while the peaks corresponding to PEG graft side chains and *tert*-butyl methacrylate segments still remained. When the *tert*-butyl methacrylate groups were replaced with carboxylic groups after the hydrolysis, the characteristic peak of *tert*-butyl methacrylate segments at δ 1.44 vanished, while the peak of PEG graft side chains at δ 3.61 still remained (Fig. 4c). These results verified the success of the selective hydrolysis reaction, which is consistent with other reports.[15] The molecular weights of the poly(MAA-*g*-EG) graft copolymers were calculated to be 15 k, 27 k, and 17 k (Table 1). A schematic illustration of the copolymers drawn to scale is given in Fig. 5.

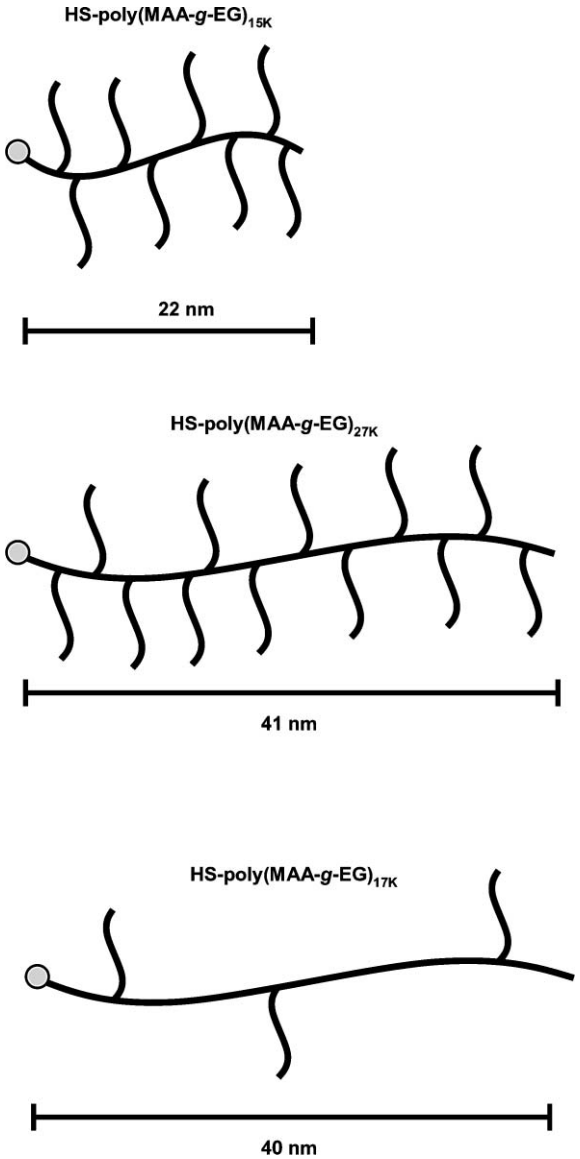

Fig. 5 Schematics of mono thiol(end)-functionalized poly(methacrylic acid-*g*-ethylene glycol) or HS-poly(MAA-*g*-EG) graft copolymers synthesized in this study with contour length dimensions for PMAA (poly(methacrylic acid)) backbone, PEG (poly (ethylene glycol)) side chains, and PEG side chain density drawn approximately to scale. The schematics are not meant to indicate the actual spatial distribution of PEG side chains along the MAA backbone or the conformation of the polymer chains. The numerical subscript in the abbreviated polymer name labels refer to the number average molecular weight, M_n, of the graft copolymer in g/mol (as measured by ^{1}H nuclear magnetic resonance) and "k" is an abbreviation for 1000.

FTIR. The FTIR spectra of HS-poly(*tert*-BMA-*g*-EG)$_{35k}$ and HS-poly(MAA-*g*-EG)$_{27k}$ (before and after hydrolysis) were obtained to additionally confirm the success of hydrolysis. As shown in Fig. 6, after hydrolysis a broad peak is observed at 2500–3500 cm^{-1} due to the formation of hydrogen bonding,[43,44] which is not possible for the HS-poly(*tert*-BMA-*g*-EG). In the spectrum of HS-poly(*tert*-BMA-*g*-EG), 2978 cm^{-1} was attributed to the asymmetric stretching of –CH_3; 1724 cm^{-1} was the stretching of C=O in the carbonyl group of *tert*-BMA; 1394 cm^{-1} and 1368 cm^{-1} was due to the bending of –CH_3 group, which are the characteristic absorptions of *tert*-butyl group,[45] 1276 cm^{-1} and 1251 cm^{-1} were the stretching of –C–C–O of PEG and 1140 cm^{-1} was attributed to the stretching of C–O.

By treatment with HCl in dioxane the *tert*-butyl groups were removed to form free carboxylic acid groups. Besides considerable absorption due to the –OH stretching of hydrogen bonding at 2500–3500 cm^{-1}, the C=O absorption peak of the MAA groups split into two peaks: 1731 cm^{-1} and 1698 cm^{-1}, which has been seen in poly(styrene-*co*-MAA)[46] and poly(MAA-*g*-EG).[47] From FTIR studies on complexes of PMAA gel with PEG,[48] the 1731 cm^{-1} would be attributed to the C=O absorption peak affected by the formation of the hydrogen bonding between PMAA and PEG side chains and the 1698 cm^{-1} would be attributed to the C=O absorption peak affected by the formation of the hydrogen bonding between two carboxylic groups of PMAA on the backbone. The FTIR spectrum of HS-poly(MAA-*g*-EG) also shows there

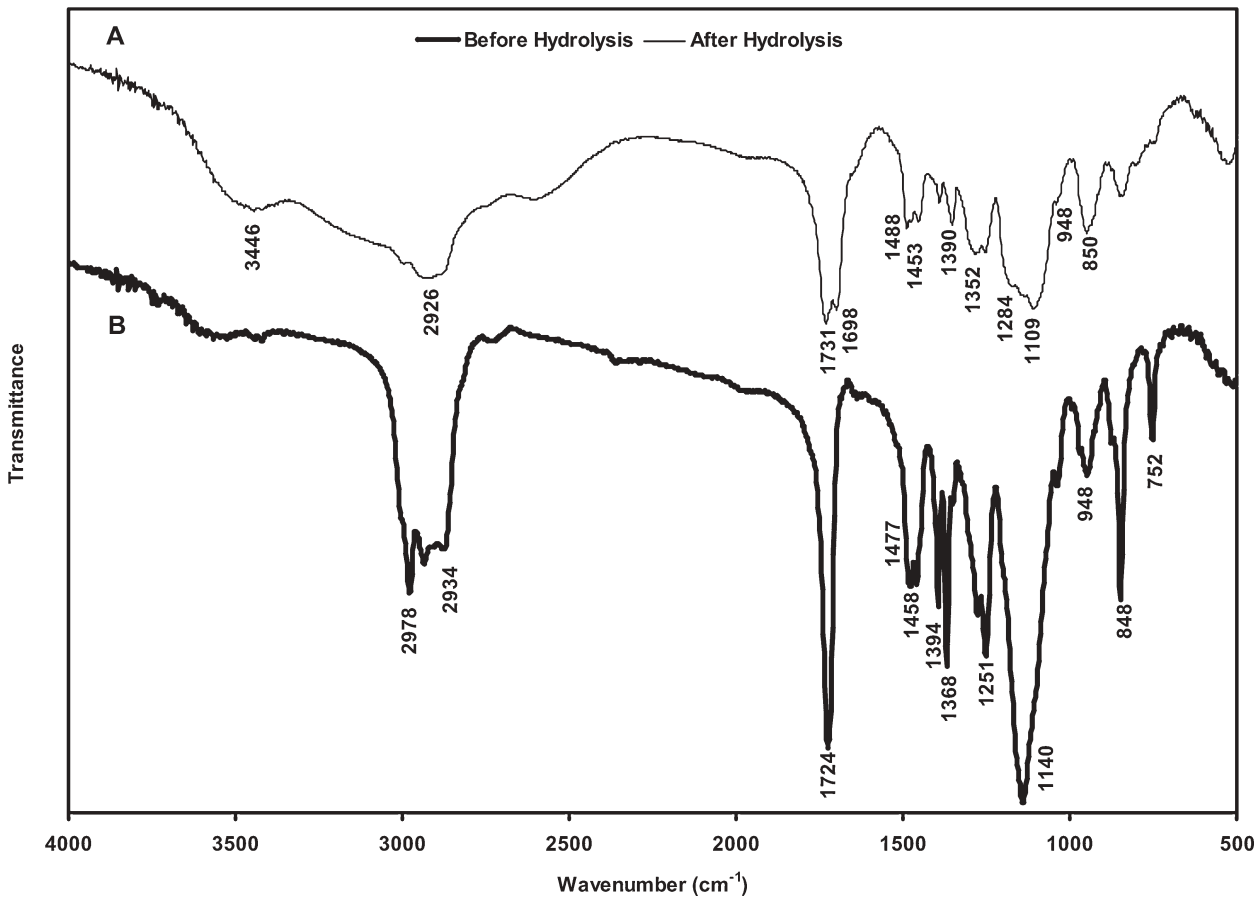

Fig. 6 Fourier transform infrared (FTIR) spectra of (a) after hydrolysis, mono thiol(end)-functionalized poly(methacrylic acid-*g*-ethylene glycol) or HS-poly(MAA-*g*-EG)$_{27k}$ and (b) before hydrolysis, mono thiol(end)-functionalized poly(*tert* butyl methacrylate-*g*-ethylene glycol) or HS-poly(*tert*-BMA-*g*-EG)$_{35k}$. The numerical subscript in the abbreviated polymer name labels refer to the number average molecular weight, M_n, of the graft copolymer in g/mol (as measured by ^{1}H nuclear magnetic resonance) and "k" is an abbreviation for 1000.

are still absorptions in the region of 1394–1368 cm^{-1}, though the peak positions shifted slightly. Since there were –CH_3 groups remaining on the backbone after the hydrolysis, 1390 cm^{-1} and 1353 cm^{-1} were attributed to symmetric bending vibrations of –CH_3 groups under the influence of acid dimers or formation of hydrogen bonding.

Solubility. The 27 k and 15 k polymers were observed to dissolve completely in pH 6, 7.1, 8 and 9 and swelled in pH 4 and 5 aqueous solutions. The 17 k polymers dissolved completely in pH 6, 7.1, 8 and 9, partially dissolved in pH 5, and swelled in pH 4.

(B) Contact angle measurements on end-grafted poly(MAA-*g*-EG)

Fig. 7 shows a dramatic decrease in advancing contact angles with chemisorption incubation time for DI water relative to the hydrophobic bare gold substrate (70 $\pm$ 2°) on end-grafted poly(MAA-*g*-EG)$_{27k}$. The instantaneous advancing contact angles equilibrated after $\sim$48 h of incubation time stabilizing at 32 $\pm$ 0.6° (27 k), 44 $\pm$ 2.4° (17 k), and 47 $\pm$ 2.6° (15 k). To achieve the highest surface grafting density, samples were prepared with an incubation time of 72 h. Receding contact angles were 0° (27 k), 5 $\pm$ 0.5° (17 k), and 11 $\pm$ 0.6° (15 k). The large difference in advancing and receding contact angles suggest that the end-grafted poly(MAA-*g*-EG) exposed its hydrophilic segments to water after dramatic molecular reorganization due to hydration for all three polymers.

(C) Estimation of packing density of end-grafted poly(MAA-g-EG)

The heights of the polymer layers were measured in air using both the μCP-contact mode AFM method and spectroscopic ellipsometry to estimate the surface packing density. From the contact mode AFM imaging, the layer thicknesses relative to the OH-SAM were found to be $\sim$0.8 nm (27 k), $\sim$1.5 nm (17 k) and $\sim$0.3 nm (15 k). The height of HS$(CH_2)_{11}$OH is known to be 1.4 $\pm$ 0.1 nm in air.[27] Hence, the dry polymer layer heights were calculated to be $\sim$2.2 nm (27 k), $\sim$2.9 nm (17 k) and $\sim$1.7 nm (15 k), which is similar to the thicknesses obtained from the ellipsometry (2.2 nm for the 27 k polymer, 2.0 nm for the 27 k polymer, and 1.4 nm for the 15 k polymer). From the AFM-measured height values, the packing densities were calculated to be $\Gamma \sim 0.053$ chains nm^{-2} or a molecular separation distance of $\sim$4.3 nm (27 k), $\Gamma \sim 0.109$ chains nm^{-2} or a molecular separation distance of $\sim$3.1 nm (17 k) and $\Gamma \sim 0.071$ chains nm^{-2} or a molecular separation distance of $\sim$3.8 nm (15 k). These values are $\sim$2$\times$ larger than the

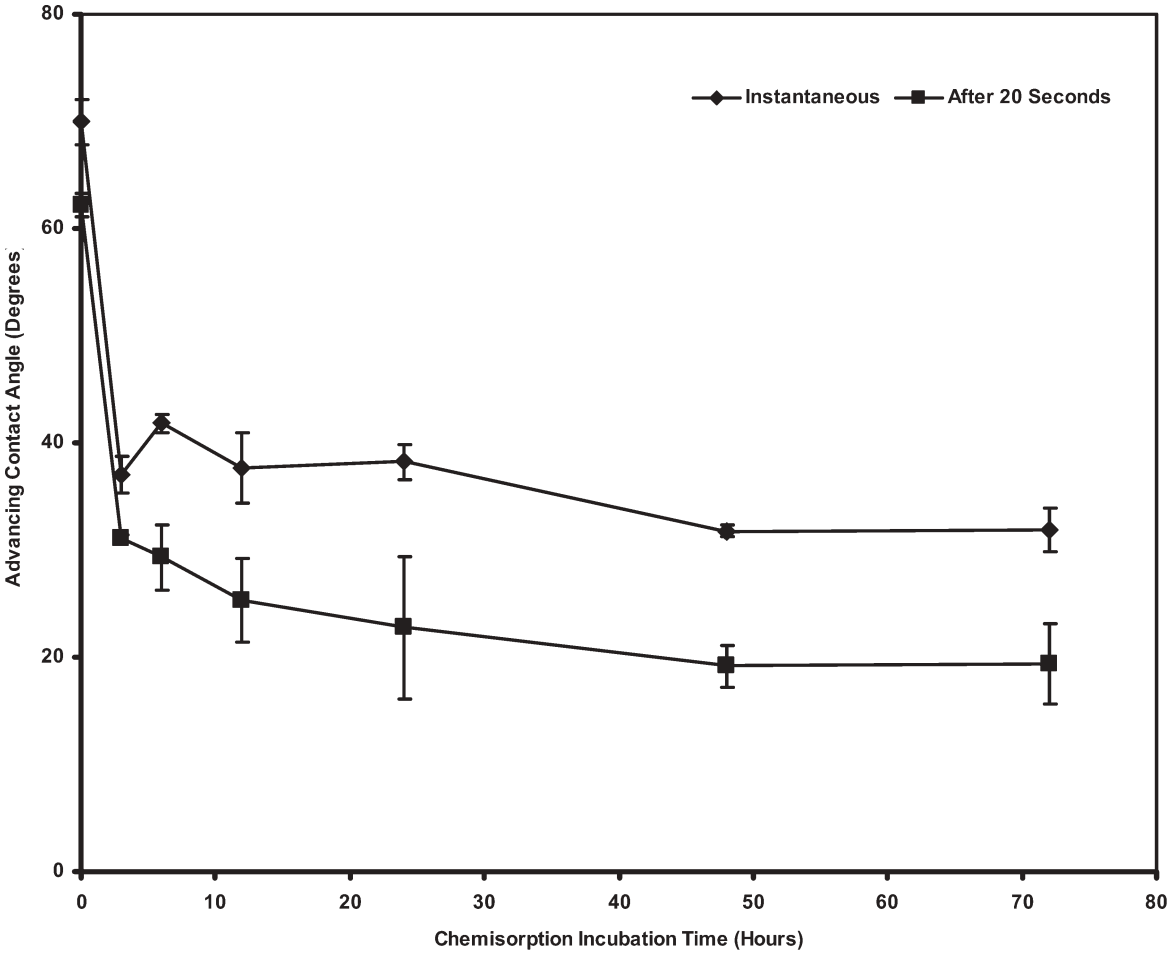

Fig. 7 Advancing contact angles of gold (zero hours) and chemically end-grafted poly(methacrylic acid-*g*-ethylene glycol) or poly(MAA-*g*-EG)$_{27k}$ layers as a function of chemisorption incubation time. The numerical subscript in the abbreviated polymer name labels refer to the number average molecular weight, M_n, of the graft copolymer in g mol^{-1} as measured by ^{1}H nuclear magnetic resonance and "k" is an abbreviation for 1000. Symbols represent the average of three different locations and hi-lo bars represent one standard deviation.

radius of gyration of these 1100 g mol^{-1} PEG side chains ($\sim$1.5 nm[49]). However, lateral interactions between PEG chains are expected at these grafting densities since PEG is known to have longer range repulsive interactions up to $\sim 3\times$ its radius of gyration.[49]

(D) Stimulus-responsive conformational transition of end-grafted poly(MAA-*g*-EG)

Fig. 8 shows contact mode AFM height images of micro-contact printed 15 k (72 h chemisorption incubation time)/OH-SAM surfaces taken under the minimum possible normal forces in a series of buffer solutions with pH 4–9 (ionic strength = 0.005 M). These images allow for direct visualization of variations in the polymer conformation, which is quantified in the subsequent height *versus* pH plot of Fig. 9. At high pH the carboxylic acid groups of PMAA are ionized (negatively charged) and unbound to the PEG chains which are free to participate in hydrogen bonding with water. Both intramolecular electrostatic repulsion and the hydrophilicity of PEG can contribute to a significant coil expansion. At pH 9, the height was found to be 8 $\pm$ 0.8 nm (0.36$L_{contour}$) for the 15 k, EG/MAA $\sim$ 2.2, 15 $\pm$ 0.5 nm (0.37$L_{contour}$) for the 27 k, EG/MAA $\sim$ 1.9, and 9.1 $\pm$ 0.4 nm (0.23$L_{contour}$) for 17 k, EG/MAA $\sim$ 0.4 polymers. These results suggest that the relative extension is determined by the side chain graft density where a lower graft density results in a lower relative extension of the main chain backbone. Since a small tare force of up to $\sim$200 pN is necessary to attain stable feedback for AFM imaging, some compression of the polymer layer may result and these AFM measured height values may be somewhat less than the true equilibrium polymer heights (depending on the nanoscale compliance of the polymer layer). At high pH values (7–9), the height of the 27 k polymer was found to be statistically larger ($p < 0.003$) than the 15 k and 17 k.

As the pH is reduced, the carboxyl groups of the PMAA become protonated and intrapolymer main-chain side-chain complexation can take place *via* hydrogen bonding with the PEG –O– groups and is thought to be further stabilized by hydrophobic interactions between the –CH_3 groups of PMAA and the hydrophobic segments of PEG. This leads to a hydrophobic, globular, collapsed conformation. As the pH is decreased, the AFM-measured height (Fig. 9) is observed to decrease gradually until reaching a minimal value of $\sim$1–2 nm

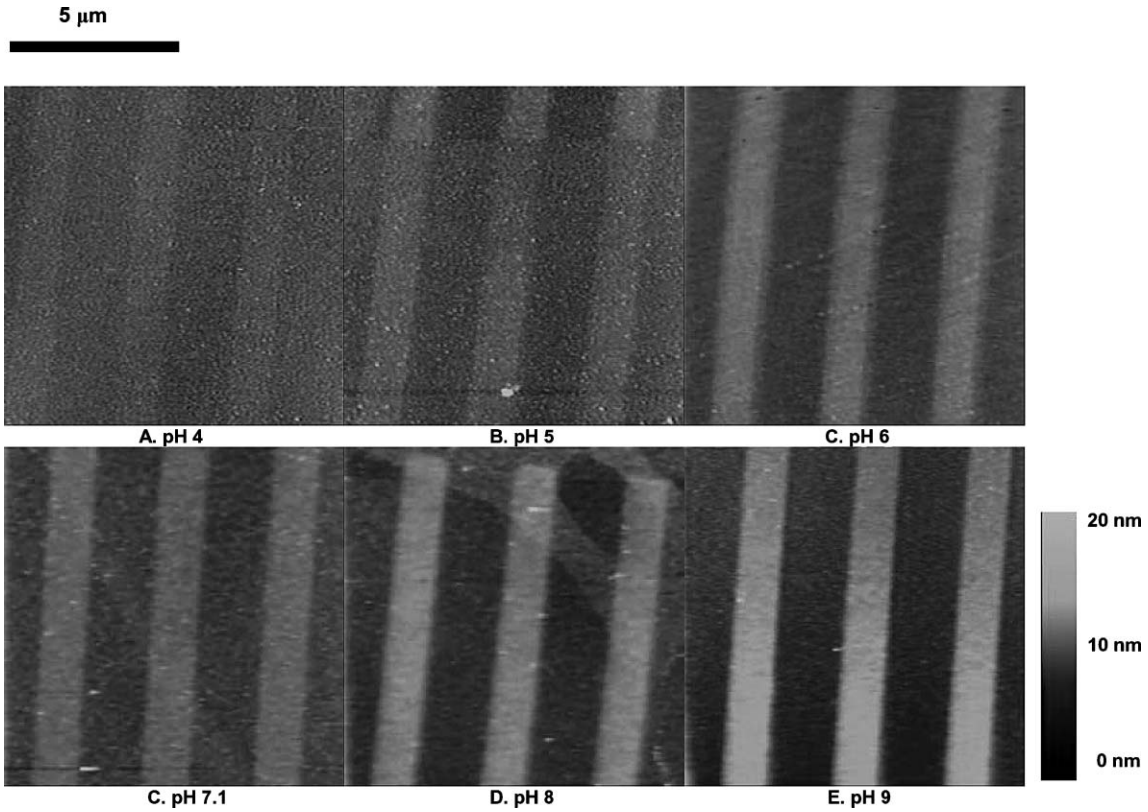

Fig. 8 AFM contact mode height images of micro-contact printed samples of end-grafted poly(methacrylic acid-*g*-ethylene glycol) or poly(MAA-*g*-EG)$_{15k}$ layers (inside the line patterns) and a hydroxy-terminated self-assembling monolayer (OH-SAM, outside the line patterns) and as a function of pH (ionic strength = 0.005 M) taken with an OH-SAM functionalized probe tip. The minimum possible normal imaging force was employed. The numerical subscript in the abbreviated polymer name labels refer to the number average molecular weight, M_n, of the graft copolymer in g mol^{-1} as measured by ^{1}H nuclear magnetic resonance and "k" is an abbreviation for 1000.

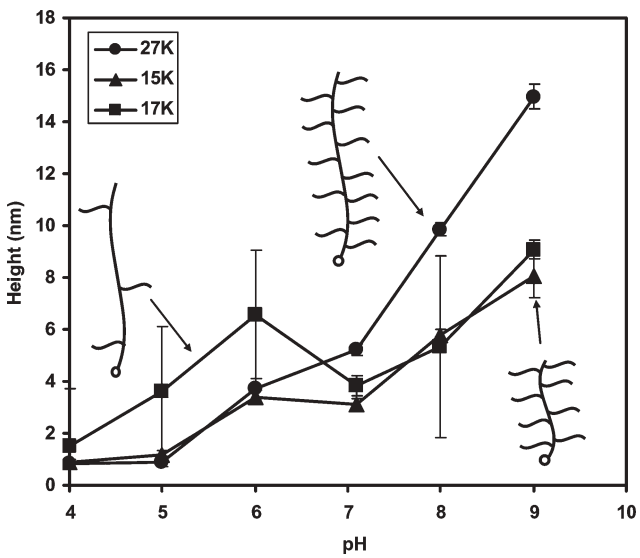

Fig. 9 Heights of end-grafted poly(methacrylic acid-*g*-ethylene glycol) or poly(MAA-*g*-EG) polymer layers relative to a hydroxy-terminated self-assembling monolayer measured by contact mode atomic force microscopy at the lowest possible imaging force as a function of pH in 0.005 M buffered aqueous solution on micro-contact printed samples. Hi-lo bars represent one standard deviation. Heights are the average of eight scan lines per image.

at pH 4, indicating that the polymer layer was in a nearly completely flattened state during imaging (height values for all three polymers were statistically similar ($p > 0.01$). Hence, the expanded to collapsed conformational transition appears to be completed between pH 4–5 which is consistent with the solubility results, reports on high MW (~700–800 K) poly(MAA-*g*-EG) in dilute aqueous solution,[14] and equilibrium swelling of macroscopic crosslinked poly(MAA-*g*-EG) hydrogels.[50] The pK_a of high MW poly(MAA-*g*-EG) has been reported between 5.8–6.7 and interestingly light scattering data on these high MW polymers show minimal expansion above pH 6.0, even though further ionization takes place.[14] In our experiment, we do not observe formation of a plateau, only continued expansion up until pH 9 (the highest pH tested), similar to the macroscopic equilibrium swelling behavior of crosslinked poly(MAA-*g*-EG) gels[50] and high molecular weight PMAA brushes.[51,52] This behavior may be indicative of intermediate conformations which has been suggested previously.[53,54] While a quantitative comparison with studies of poly(MAA-*g*-EG) in dilute gel form[14,50] is not possible due to differences in copolymer and PEG MW, solution ionic strength, and sample type, it is interesting to note that many qualitatively similar trends emerge. The height of the 17 k polymer at lower pH values (5–6) was statistically greater than the 27 k or 15 k polymer ($p < 0.015$). It is noted that the

surfaces are still extremely hydrophilic at pH 5.6 (as indicated by contact angle measurements taken with DI water) when the polymer layers have already collapsed by 70–85% of its expanded height at pH 9, suggesting that wettability should have a much more discrete stimulus-responsive nature.

Fig. 10a is a plot of the heights of the poly(MAA-*g*-EG) layers measured by contact mode atomic force microscopy as a function of normal imaging force on micro-contact printed samples in buffered aqueous solution of pH 9 and ionic strength of 0.005 M. A nonlinear decrease in polymer height is observed for both molecular weights with increasing normal force until reaching a plateau value ("incompressible layer height") of <2 nm at ~10 nN of force. Fig. 10b shows the corresponding data for pH 4 where all three polymers are in a nearly completely collapsed configuration.

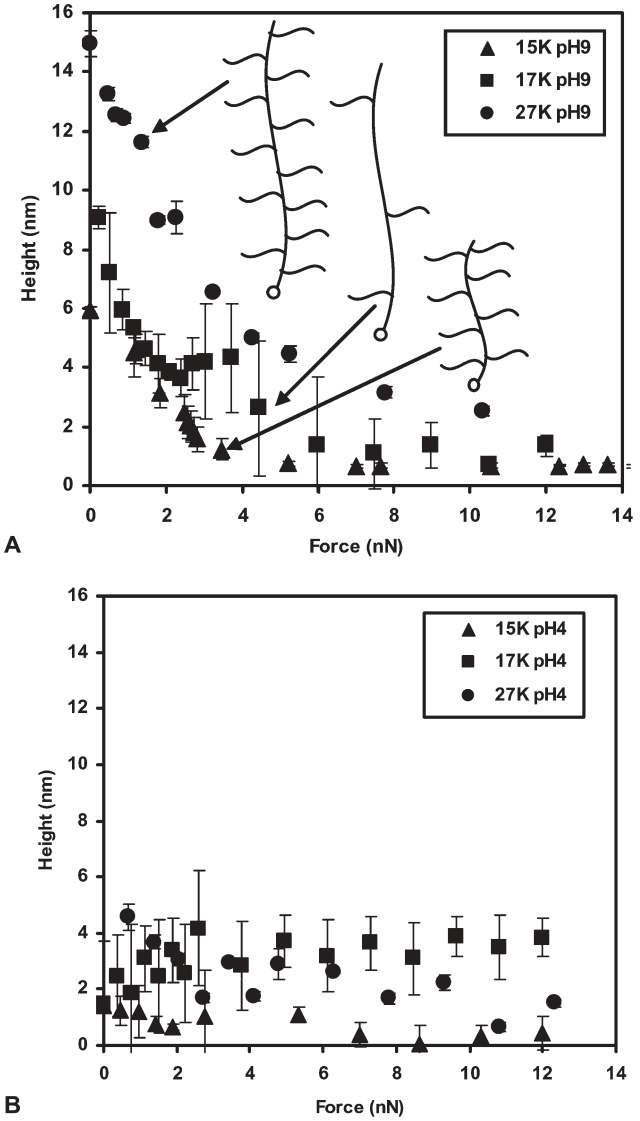

Fig. 10 Heights of end-grafted poly(methacrylic acid-*g*-ethylene glycol) or poly(MAA-*g*-EG) polymer layers relative to a hydroxy-terminated self-assembling monolayer measured by contact mode atomic force microscopy as a function of normal imaging force in 0.005 M buffered aqueous solution on micro-contact printed samples. Hi-lo bars represent one standard deviation. Heights are the average of eight scan lines per image. (a) pH 9 and (b) pH 4.

(E) Comparison of end-grafted poly(MAA-*g*-EG) layers to other reported end-grafted stimulus-responsive macromolecular systems

One parameter that can be employed to directly characterize the magnitude of the stimulus responsive nature of a particular system is a swelling factor, *s*, which for end-grafted macromolecular layers exposed to a particular stimulus can be defined as:

$$s = \frac{\text{maximum height}}{\text{minimum height}}$$

where the heights may be taken anywhere throughout the stimulus range. *s* is expected to depend on Γ and intermolecular interactions, DP_n and polydispersity, macromolecular architecture and intramolecular interactions, and surface curvature. *s* is also expected to decrease at high grafting densities due to lateral confinement effects and layer stiffening. Values of *s* have been observed to be exceedingly large (up to 19) for polyelectrolytes attached to curved surfaces (calculated by hydrodynamic thicknesses measured by dynamic light scattering of brush-functionalized particle dispersions), for example; temperature and salt concentration of poly(N-isopropylacrylamide) (PNIPAM),[55] pH and salt concentration dependence of polyacrylic acid or PAA, salt concentration dependence for poly(2-(dimethylamino)ethyl methacrylate) or PDMAEMA[56] and salt concentration dependence of poly(styrene sulfonate) or PSS.[57] Hence, for consistency we will limit further discussion to macromolecules attached to planar surfaces. Table 2 provides a summary of end-grafted or end-anchored PAA[59,60] and PMAA[51,52,58] data reported in the literature compared to the poly(MAA-*g*-EG) graft copolymers studied here. *s* values are measured to be <3.3 for PAA and PMAA with a wide variety of DP_n and grafting densities while *s* for the poly(MAA-*g*-EG) were found to be generally larger at 4.14 (15 k), 3.64 (17 k), and 7.3 (27 k). The swelling factors calculated for the poly(MAA-*g*-EG) were from low force contact mode AFM imaging of μCP samples while the majority of the others were measured *via* ellipsometry. As mentioned before, the former method (AFM) typically will leads to an underestimation of the measured heights, which would in turn lead to an underestimation of *s* and hence, the trend observed comparing poly(MAA-*g*-EG) to PAA and PMAA can not be due to differences in the measurement techniques.

To compare these values to other types of stimuli, PAA and PMAA also exhibit a well-known nonmonotonous dependency on salt concentration which exhibits a maximum height between the "osmotic brush" and "salted brush" regimes.[59] Swelling factors as a function of salt concentration for PAA and PMAA are generally larger than for pH dependency of the equivalent systems ($s \sim 1.4$–6.4).[51,52,59,60] Solvent and temperature-dependent swelling factors for end-grafted poly(*N*-isopropylacrylamide) (PNIPAM) on planar substrates are found to be <3.2.[61–64] Other end-tethered stimulus-responsive macromolecular layers reported in the literature (which did not report heights and swelling factors) include; elastin-like polypeptides,[65] semifluorinated polystyrene and poly(methyl acrylate)-based diblock copolymers,[66] binary layers of chemically modified poly(styrene)/poly(methyl acrylate), poly(butyl acrylate) or poly(acrylic acid),[67,68] and Y-shaped amphiphilic poly(styrene)/poly(acrylic acid).[69,70] In

Table 2 Summary of swelling factors for heights of poly(acrylic acid) or PAA and poly(methacrylic acid) or PMAA end-anchored or chemically end-grafted weak polyelectrolyte layers as a function of pH compared to poly(methacrylic acid-*g*-ethylene glycol) or poly(MAA-*g*-EG) reported in this paper where the swelling factor, *s*, is defined as the maximum height divided by the minimum height, Γ is the grafting density (chains nm^{-2}), DP_n is the number average degree of polymerization, and μCP is micro contact printing. *s* for the poly(MAA-*g*-EG) was calculated with the addition of 1.4 nm[27] to each of the heights since the reported values (Fig. 9) were relative to the $SH(CH_2)_{11}OH$ self-assembling monolayer.

Polymer	DP_n	Γ/chains nm^{-2}	Technique	*s*	Reference
PAA[b]	49–57	0.1–0.86	Ellipsometry	<1.28	Wu *et al.*[59]
PAA[a]	122	0.125–0.39	Ellipsometry	<2.35	Currie *et al.*[60]
PMAA[b]	300	—	AFM (scratch method)	1.97	Ryan *et al.*[58]
PMAA[b]	High[c]	—	Ellipsometry	3.3	Konradi *et al.*[51]
PMAA[b]	23 000	0.005–0.16	Ellipsometry	1.9–2.5	Zhang *et al.*[52]
poly(MAA-*g*-EG)[b]	80–155	0.053–0.11	AFM (μCP)	3.6–7.3	This study

[a] End-anchored. [b] Chemically end-grafted. [c] The DP_n in Konradi, *et al.*[51] was not reported but expected to be very large since the collapsed height of the layer at low pH was ~600 nm.

these systems and some of the others cited above, alternative surface properties have been employed to characterize stimulus responsiveness including wettability,[66,69,71] protein adsorption,[65] membrane permeability,[72] nanoscale morphology in air,[66–70] bioadhesion,[64] and more recently, nanomechanical properties.[65,67,70]

Conclusions

The three most significant contributions of this paper are as follows:

(1) The formation of stimulus-responsive chemically end-grafted "brush-brushes" by synthesizing, mono thiol(end)-functionalized poly(MAA-*g*-EG) comb-type graft copolymers *via* a combination of protecting group chemistry and atom transfer radical polymerization using the initiator 2-(2,4-dinitrophenylthio)ethyl 2-bromo-2-methyl propionate was carried out. pH-Dependent swelling was confirmed to take place gradually above pH 4–5 and quantified by contact mode AFM measurements of polymer height on μCP samples. Not only is this advance technologically important for preparing homogeneous and stable stimulus-responsive surfaces, but provides a system for which the fundamental nanoscale origins of the stimulus responsive nature of such macromolecules can be studied systematically.

(2) The synthesis of end-functionalized comb-like copolymers with varying macromolecular architecture and the assessment of its effect on the stimulus responsive transition was accomplished. Decreasing molecular weight by ~2× and side chain graft density by ~4× resulted in a decrease in swelling factor by ~2×.

(3) Measurement of the nanoscale compressibility as a function of macromolecular architecture and pH was completed. Polymer layer height *versus* normal AFM imaging force measured on μCP samples at pH 9 showed a nonlinear relationship and near-complete compression <2 nm for forces >10 nN. The 27 k polymer was observed to be the least compressible at pH 9 and at pH 4 all polymers were collapsed and essentially incompressible.

Acknowledgements

The authors wish to thank NSF-PECASE (0094194), NSF-NIRT (0403903), and a 3M innovation fund for financial support, as well as Professor Anne M. Mayes' group (Department of Materials Science and Engineering at MIT) for providing GPC assistance.

References

1 T. P. Russell, *Science*, 2002, **297**, 964–967.
2 I. Y. Galaev and B. Mattiasson, *Trends Biotechnol.*, 1999, **17**, 335–340.
3 R. Dagani, *Chem. Eng. News*, 1995, **73**, 30–33.
4 N. Nath and A. Chilkoti, *Adv. Mater.*, 2002, **14**, 1243–1247.
5 C. de las Heras Alarcon, S. Pennadam and C. Alexander, *Chem. Soc. Rev.*, 2005, **34**, 276–285.
6 S. Qin, K. Matyjaszewski, H. Xu and S. S. Sheiko, *Macromolecules*, 2003, **36**, 605–612.
7 R. Djalali, S.-Y. Li and M. Schmidt, *Macromolecules*, 2002, **35**, 4282–4288.
8 G. Cheng, A. Böker, M. Zhang, G. Krausch and A. H. E. Müller, *Macromolecules*, 2001, **34**, 6883–6888.
9 S. Desvergne, V. Heroguez, Y. Gnanou and R. Borsali, *Macromolecules*, 2005, **38**, 2400–2409.
10 D. Heinegard and A. Oldberg, *FASEB J.*, 1989, **3**, 2042–2051.
11 R. Bansil, E. Stanley and J. T. LaMont, *Annu. Rev. Physiol.*, 1995, **57**, 635–657.
12 A. M. Mathur, B. Drescher, A. B. Scranton and J. Klier, *Nature*, 1998, **392**, 367–370.
13 A. S. Restrepo and L.-K. Ju, *Ind. Eng. Chem. Res.*, 2003, **42**, 4296–4302.
14 G. D. Poe, W. L. Jarrett, C. W. Scales and C. L. McCormick, *Macromolecules*, 2004, **37**, 2603–2612.
15 M.-C. Jones, M. Ranger and J.-C. Leroux, *Bioconjugate Chem.*, 2003, 774–781.
16 M. Ye, D. Zhang, L. Han and C. Ortiz, *in preparation*, 2006.
17 D. Dean, L. Han, C. Ortiz and A. J. Grodzinsky, *Macromolecules*, 2005, **38**, 4047–4049.
18 D. Dean, L. Han, A. J. Grodzinsky and C. Ortiz, *J. Biomech.*, 2005, DOI: 10.1016/j.jbiomech.2005.09.007.
19 B. Kim and N. A. Peppas, *Polymer*, 2003, **44**, 3701–3707.
20 D. Zhang and C. Ortiz, *Macromolecules*, 2004, **37**, 4271–4282.
21 G. Carrot, J. G. Hilborn, M. Trollsas and J. L. Hedrick, *Macromolecules*, 1999, **32**, 5264–5269.
22 G. Carrot, J. Hilborn, J. L. Hedrick and M. Trollsas, *Macromolecules*, 1999, **32**, 5171–5173.
23 S. Shaltiel, *Biochem. Biophys. Res. Commun.*, 1967, **29**, 178–183.
24 J. L. Wilbur, A. Kumar, E. Kim and G. M. Whitesides, *Adv. Mater.*, 1994, **6**, 600–604.
25 D. Zhang, C. Macias and C. Ortiz, *Macromolecules*, 2005, **38**, 2530–2534.
26 J. Seog, D. Dean, A. H. K. Plaas, S. Wong-Palms, A. J. Grodzinsky and C. Ortiz, *Macromolecules*, 2002, **35**, 5601–5615.
27 A. Ulman and N. Tillman, *Langmuir*, 1989, **5**, 1418–1420.
28 C. L. Bell and N. A. Peppas, *Biomaterials*, 1996, **17**, 1203–1218.
29 K. Matyjaszewski and J. Xia, *Chem. Rev.*, 2001, **101**, 2921–2990.
30 R. Krishnan and K. S. V. Srinivasan, *Eur. Polym. J.*, 2004, **40**, 2269–2276.
31 C. Wang, P. Ravi, K. C. Tam and L. H. Gan, *J. Phys. Chem. B*, 2004, **108**, 1621–1627.

32 S. Karanam, H. Goossens, B. Klumperman and P. Lemstrat, *Macromolecules*, 2003, **36**, 3051–3060.
33 X. S. Wang and S. P. Armes, *Macromolecules*, 2000, **33**, 6640–6647.
34 X. S. Wang, F. L. G. Malet, S. P. Armes, D. M. Haddleton and S. Perrier, *Macromolecules*, 2001, **34**, 162–164.
35 G. Coullerez, A. Carlmark, E. Malmstrom and M. Jonsson, *J. Phys. Chem. A*, 2004, **108**, 7129–7131.
36 S. Perrier, S. P. Armes, X. S. Wang, F. Malet and D. M. Haddleton, *J. Polym. Sci., Part A: Polym. Chem.*, 2001, **39**, 1696–1707.
37 D. Neugebauer, Y. Zhang, T. Pakula, S. S. Sheiko and K. Matyjaszewski, *Macromolecules*, 2003, **36**, 6746–6755.
38 V. P. Sant, D. Smith and J.-C. Leroux, *J. Controlled Release*, 2004, **97**, 301–312.
39 M. Ranger, M.-C. Jones, M.-A. Yessine and J.-C. Leroux, *J. Polym. Sci., Part A: Polym. Chem.*, 2001, **39**, 3861–3874.
40 R. Krishnan and K. S. V. Srinivasan, *J. Macromol. Sci., Pure Appl. Chem.*, 2005, **A42**, 495–508.
41 M. M. Ali and H. D. H. Stover, *Macromolecules*, 2004, **37**, 5219–5227.
42 R. Begum and H. Matsuura, *J. Chem. Soc., Faraday Trans.*, 1997, **93**, 3838–3848.
43 Z. Fang and J. P. Kennedy, *J. Polym. Sci., Part A: Polym. Chem.*, 2002, **40**, 3662–3678.
44 S.-K. Kwon, W.-J. Choi, Y.-H. Kim and S.-K. Choi, *Bull. Korean Chem. Soc.*, 1992, **13**, 479–482.
45 H. S. Shin, Y. M. Jung, J. Lee, T. Chang, Y. Ozaki and S. B. Kim, *Langmuir*, 2002, **18**, 5523–5528.
46 C. S. Cleveland, K. S. Guigley, P. C. Painter and M. M. Coleman, *Macromolecules*, 2000, **33**, 4278–4280.
47 R. K. Drummond, J. Klier, J. A. Alameda and N. A. Peppas, *Macromolecules*, 1989, **22**, 3816–3818.
48 O. E. Philippova, N. S. Karibyants and S. G. Starodubtzev, *Macromolecules*, 1994, **27**, 2398–2401.
49 M. A. Rixman, D. Dean and C. Ortiz, *Langmuir*, 2003, **19**, 9357–9372.
50 F. Madsen and N. A. Peppas, *Biomaterials*, 1999, **20**, 1701–1708.
51 R. Konradi, H. Zhang, M. Biesalski and J. Rühe, in *Polymer Brushes*, ed. R. Advincula, B. Brittain, K. Caster and J. Rühe, Wiley-VCH, Weinheim, Germany, 2004; pp 249–270.
52 H. Zhang and J. Rühe, *Macromolecules*, 2005, **38**, 4855–4860.
53 S. Holappa, L. Kantonen, F. M. Winnik and H. Tenhu, *Macromolecules*, 2004, **37**, 7008–7018.
54 V. V. Khutoryanskiy, A. V. Dubolazov, Z. S. Nurkeeva and G. A. Mun, *Langmuir*, 2004, **20**, 3785–3790.
55 J. N. Kizhakkedathu, R. Norris-Jones and D. E. Brooks, *Macromolecules*, 2004, **37**, 734–743.
56 R. D. Wesley, T. Cosgrove, L. Thompson, S. P. Armes, N. C. Billingham and F. L. Baines, *Langmuir*, 2000, **16**, 4467–4469.
57 X. Guo and M. Ballauff, *Phys. Rev. E: Stat. Phys., Plasmas, Fluids, Relat. Interdiscip. Top.*, 2001, **64**, 051406/1-0514/9.
58 A. J. Ryan, C. J. Crook, J. R. Howse, P. Topham, R. A. L. Jones, M. Geoghegan, A. J. Parnell, L. Ruiz-Perez, S. J. Martin, A. Cadby, A. Menelle, J. R. P. Webster, A. J. Gleeson and W. Bras, *Faraday Discuss.*, 2005, **128**, 55–74.
59 T. Wu, P. Gong, J. Genzer, I. Szleifer, P. Vlcek and V. Šubr, in *Polymer Brushes*, ed. B. Brittain, R. Advincula, J. Rühe and K. Caster, Wiley & Sons, Weinheim, Germany, 2003.
60 E. P. K. Currie, A. B. Sieval, G. J. Fleer and M. A. C. Stuart, *Langmuir*, 2000, **16**, 8324–8333.
61 M. Kaholek, W.-K. Lee, B. LaMattina, K. Caster and S. Zauscher, In *Polymer Brushes*, ed. R. Advincula, B. Brittain, K. Caster and J. Rühe, Wiley-VCH, Weinheim, Germany, 2004, pp 381–402.
62 M. Kaholek, W.-K. Lee, B. LaMattina, K. C. Caster and S. Zauscher, *Nano Lett.*, 2004, **4**, 373–376.
63 M. Kaholek, W.-K. Lee, S.-J. Ahn, H. Ma, K. C. Caster, B. LaMattina and S. Zauscher, *Chem. Mater.*, 2004, **16**, 3688–3696.
64 C. de las Heras Alarcon, T. Farhan, V. L. Osborne, W. T. S. Huck and C. Alexander, *J. Mater. Chem.*, 2005, **15**, 2089–2094.
65 J. Hyun, W.-K. Lee, N. Nath, A. Chilkoti and S. Zauscher, *J. Am. Chem. Soc.*, 2004, **126**, 7330–7335.
66 A. M. Granville, S. G. Boyes, B. Akgun, M. D. Foster and W. J. Brittain, *Macromolecules*, 2005, **38**, 3263–3270.
67 M. Lemieux, D. Usov, S. Minko, M. Stamm, H. Shulha and V. V. Tsukruk, *Macromolecules*, 2003, **36**, 7244–7255.
68 M. C. LeMieux, D. Julthongpiput, K. N. Bergman, P. D. Cuong, H.-S. Ahn, Y.-H. Lin and V. V. Tsukruk, *Langmuir*, 2004, **20**, 10046–10054.
69 D. Julthongpiput, Y.-H. Lin, J. Teng, E. R. Zubarev and V. V. Tsukruk, *Langmuir*, 2003, **19**, 7832–7836.
70 Y.-H. Lin, J. Teng, E. R. Zubarev, H. Shulha and V. V. Tsukruk, *Nano Lett.*, 2005, **5**, 491–495.
71 S. Balamurugan, S. Mendez, S. S. Balamurugan, M. J. O'Brien II and G. P. Lopez, *Langmuir*, 2003, **19**, 2545–2549.
72 H. Zhang and Y. Ito, *Langmuir*, 2001, **17**, 8336–8340.